

Geological study on the formations of grooves on Phobos: Results of image analysis

Hiroshi Kikuchi^{1*}, Hideaki Miyamoto¹

¹The University Museum, The University of Tokyo

Phobos and Deimos have been imaged by Viking orbiter, HRSC onboard Mars Express, and HiRISE onboard Mars Reconnaissance orbiter. About 3000 high-resolution images of Phobos have been acquired, which indicates that Phobos becomes one of the most densely-imaged small solar system bodies. The purpose of our study is to understand formational and evolutionary processes of small bodies through image analysis.

One of the most distinguished features on the surface of Phobos is the lineally surface structure, which is most commonly called as a groove. Grooves are found on many small solar system bodies, however, their formational processes has not been explained.

Some formational processes of grooves on Phobos have been proposed, such as (1) the faults vents caused by tectonic forces [1] and (2) the secondary craters due to a large impact on either Phobos or Mars [2]. However, neither hypothesis satisfies findings from all of the observational or theoretical studies.

In this study, we carefully analyze high-resolution images of Phobos and identified 515 grooves, whose locations are carefully mapped out on the numerical shape-model of Phobos. At a result, we find that many grooves have rims, which support the view that the grooves on Phobos are related to impact events. We also make a histogram of the lengths of the grooves, where those more than 5km can produce reliable information.

We also map the locations of craters more than 20km in diameter on three regions to determine the crater densities, which are below geometric saturation at any regions. In particular the high-latitude region has a low crater density. We find that the crater size frequency on sub-Mars is similar to that on Anti-Mars. We also map the distributions and the size of boulders on the surface. As a result, the size of many boulders is about 20m diameter, and many boulders can be identified on the equatorial region. Additionally we discover ridges whose formative factor cannot be explained. These analysis results deny existing hypotheses. In this presentation, we will show our new hypothesis that the origin of grooves is the impact from asteroids can explain these analysis results coherently.

Reference

- [1] Soter, S. and Harris, A., 1978. *Nature* 268, 421-422
- [2] Murray, J.B., Iliffe, J.C., 2011. *Geomorphology. Geol. Soc. Spec. Publ.*, London, pp.21-41
- [3] Kenneth, R.R., James, W. H., 2013. *Planetary and Space Science*, 69-95

Numerical models of thermal convection in the mantle of super-Earths

Chihiro Tachinami¹, Masaki Ogawa^{2*}, Masanori Kameyama³

¹Department of Earth Planetary Sciences, Tokyo Institute of Technology, ²Department of Earth Science and Astronomy, University of Tokyo at Komaba, ³Geodynamic Research Center, Ehime University

Numerical models are developed for thermal convection of compressible fluid in a deep mantle with the ratio of its depth to the thermal scale height D much larger than 1 to understand the nature of mantle convection in super-Earths. The viscosity is constant and the Prandtl number is infinite. A linear stability analysis shows that thermal convection is possible in super-Earths only when the thermal expansivity significantly decreases with increasing pressure, as is the case for the real mantle materials; thermal convection is totally inhibited when the thermal expansivity is constant. A systematic numerical simulation carried out to clarify the Nusselt number-Rayleigh number relationship shows that the efficiency of convective heat transport decreases by a factor of up to 2 as D increases. The Nusselt number may not be high enough to extract all the heat generated in the mantle by heat producing elements, and it may be difficult to sustain core-dynamo in super-Earths. Our numerical experiments also show that the Nusselt number significantly depends on the surface temperature. The mantle evolution may depend more strongly on the surface environment in super-Earths than it does in the terrestrial planets of our solar system.

Keywords: super-Earth, mantle convection, adiabatic compression, numerical simulation

Rheological structure in Venus and implication to its surface tectonics

Shintaro Azuma^{1*}, Ikuo Katayama¹, Tomoeki Nakakuki¹

¹Hiroshima University, Department of Earth and Planetary Systems Science

Venus has been regarded as a twin planet to the Earth, because of density, mass, size and distance from the Sun. However, the Magellan mission revealed that plate tectonics is unlikely to work on the Venus [1][2]. The plate tectonics is one of the most important mechanism of heat transport and material circulation of the Earth, consequently, its absence might cause the different tectonic evolution between Earth and Venus. Rheological structure is a key to inferring mantle structure and convection style of planet interiors because the rock rheology controls strength and deformation mechanism. In previous study, the behavior of Venusian lithosphere has been inferred from the power-law type flow law of dry diabase [3]. They indicated that lower crust can be weaker than upper mantle, which might result decoupling at the crust-mantle boundary (Moho depth) and mantle convection without crustal entrainment. However, the power-law creep cannot be applicable to infer the rheological structure at Moho depths, because the dislocation-glide control creep (Peierls mechanism) is known to become dominant at relatively low temperatures in materials with a relatively strong chemical bonding such as silicates [4]. In this study, we conduct two-phase deformation experiments to directly investigate rheological contrast between plagioclase (crust) and olivine (mantle) and discuss the difference between these planets in terms of rheological behaviors. Moreover, one-dimensional numerical calculation is performed to evaluate the influence of strength contrast to the decoupling of deformation rate at the Moho. Our experiments using solid-medium deformation apparatus directly determine the relative strength between plagioclase (crust) and olivine (mantle) without any extrapolating of flow law. The experimental conditions were ranging 2GPa and 600-1000 degrees under dry conditions. In one-dimensional numerical calculation, three models were prepared; each model is distinguished in rheological structure. First model has no strength contrast at Moho, second and third models have double-digit difference and four-digit difference in viscosity each at Moho. And we observed difference of the surface velocity at each model when it is assumed that the velocity at the bottom (100km depth) is 20 cm/year and stress value is constant (=100MPa) at each depth in calculations.

The experimental results show that olivine is expected to always be stronger than plagioclase. This result contradicts to that inferred from power-law creep of olivine and plagioclase, suggesting that Peierls mechanism could be dominant deformation mechanism in both olivine and plagioclase at relatively low temperatures. In the case of the Earth, rheological structure of oceanic lithosphere is constrained well by Byerlee's law and power-law type flow law [5]. The oceanic crust and mantle lithosphere are strongly coupled mechanically because the Moho has no strength contrast, so that they could move and subduct together into the deep. In contrast, our experimental results imply that large strength contrast exists at Moho in Venus, resulting decouple of the motion between the crust and mantle lithospheres because the weak lower crust acts as a lubricant. Also one-dimensional numerical calculations show us that the surface velocity becomes more sluggish in the model which has larger strength contrast (from two-digit to four-digit difference in viscosity) at Moho. Therefore the crustal part is less likely to be involved to mantle convection when strength contrast gets larger and larger. [1] Kaula, W. M. & Phillips, R. J., *Geophys. Res. Lett.* 8, 1187 (1981). [2] Turcotte D. L., Morein G., Roberts D., & Malamud B. D., *Icarus* 139, 49-54 (1999). [3] Mackwell, S. J., Zimmerman, M.E. & Kohlstedt, D.L., *J. Geophys. Res.* 103, 975-984 (1998). [4] Tsenn, M. C. & Carter, N. L., *Tectonophys.* 136, 1-26 (1987). [5] Kohlstedt, D. L., Evans, B. & Mackwell, S. J., *J. Geophys. Res.* 100, 17,587-17,602 (1995).

Keywords: plagioclase, olivine, venus, relative strength, deformation experiment, tectonics

Laser shock compression experiments for precompressed Methane in Mbar regime

Tsuyoshi Ogawa^{1*}, Norimasa Ozaki¹, Marius Millot³, Takayoshi Sano², Yuto Asami¹, Syotaro Iketani¹, Hiroyuki Uranishi¹, Mika Kita¹, Yoshihiko Kondo¹, Yuya Sato¹, Kazuki Nakatsuka¹, Kohei Miyanishi¹, Yang Tsung-Han¹, Raymond Jeanloz³, Burkhard Militzer³, Gilbert W. Collins⁴, J. Ryan Rygg⁴, Jon H. Eggert⁴, Philip Sterne⁴, Youichi Sakawa², Ryosuke Kodama¹

¹Graduate School of Engineering, Osaka University, ²Institute of Laser Engineering, Osaka University, ³University of California Berkeley, ⁴Lawrence Livermore National Laboratory

The properties of methane at high density and temperature are of crucial interest for understanding the interiors of many giant planets, and the origin of their strong magnetic fields, as CH₄ is typically considered to represent 25 % of the planet's icy layer. Methane is a hydrogen-rich molecular material that is expected to dissociate at high pressure and temperature into an electrically conductive fluid.

We used static and dynamic coupling compression technique to generate icy planets core conditions in laboratory.

Methane was precompressed to ~0.4 GPa by DAC and then was shock compressed dynamically to pressures of more than 100 GPa.

We simultaneously measured pressure, density, temperature, and optical reflectivity for the highly compressed methane with velocity interferometers (VISAR) and optical pyrometer (SOP).

This work was performed under the joint research project of the ILE, Osaka University.

This work was partially supported by grants from the Core-to-Core Program of the JSPS, the Global COE Program CEDI of the MEXT, and the CREST of the JST.

Keywords: High-Power Laser, static and dynamic coupling compression, Methane, DAC

Physical properties of water and alcohol?water mixtures in the transition region between ionic fluid and plasma

Mika Kita^{1*}, Norimasa Ozaki¹, OKUCHI, Takuo², KIMURA, Tomoaki³, SANNO, Takayoshi², SAKAWA, Youichi², KODAMA, Ryosuke¹

¹Grad. school of Eng., Osaka Univ., ²Institute for Study of the Earth's Interior, Okayama Univ., ³Geodynamics Research Center, Ehime Univ., ⁴Institute of Laser Engineering, Osaka Univ.

Mixtures of water, methane, and ammonia at high pressures and temperatures are thought to be the major constituents of Ice Giants like Uranus and Neptune. Understanding of composition and formation of these planets relies on the existing equation-of-state (EOS) of the elements and compounds. However, these EOS and properties near phase boundaries (e.g. ionic fluid to plasma), where its physical and chemical properties are changing dramatically, have not known well. In order to understand planetary chemistry, laboratory measurements of the material properties are required in the transition regime.

We performed laser-shock compression experiments for liquid specimens to pressures of more than 100 GPa. We measured shock velocities, optical reflectivity, and shock temperature by using Velocity Interferometer System for Any Reflector (VISAR) and Streaked Optical Pyrometer (SOP). These experimental observables are compared between pure water and ethyl alcohol/water mixtures in the transition pressure-temperature regime. Optical reflectivity of the mixture is significantly higher than of water. We here discuss the effect of carbon ions on the mixture reflectivity.

This work was performed under the joint research project of the ILE, Osaka University. This work was partially supported by grants from the Core-to-Core Program of the JSPS, the Global COE Program CEDI of the MEXT, and the CREST of the JST.

Keywords: ice giants, water, mixture, phase transition, laser shock compression, equation of state

Orbital Evolution of Centaurs and their activity

Arika Higuchi^{1*}, Takeru Kobayashi¹, Shigeru Ida¹

¹Tokyo Institute of Technology

We have investigated the orbital evolution of Centaurs and their cometary activity.

According to the orbital integrations by many authors, Centaurs are thought to be objects that are transitioning between the Kuiper Belt region and the inner solar system. Due to the strong perturbations from giant planets, Centaurs have short dynamical lifetime of $\sim 10^7$ years: about two-thirds are ejected from the solar system and one third are injected into the inner region to be called Jupiter family comets (e.g., Volk&Malhotra 2008.) According to Jewitt (2009), 16 active Centaurs have been found. It is curious that some of such Centaurs show cometary activity. Their activity cannot be explained as an ordinal water sublimation of short-period comets since they are too cold for water sublimation to be effective and also too hot to keep CO ice. The alternative mechanism of their activity has been proposed and discussed in Jewitt (2009). Jewitt said that if Centaurs contain the amorphous ice that is porous and have enough space to keep CO gas, the CO outgassing occurs when the amorphous ice transforms into crystalline form. Observations of Centaurs support the hypotheses that the crystallization of amorphous ice (thermal process) is the trigger or driver of activity. But we have no idea how long the activity maintained. Guilbert (2012) calculated the 3-D thermal evolution of icy body due to the heat from the Sun in detail, including the seasonal variation. She found that the crystallization of amorphous ice is completed in 10^4 -5 years. However, Guilbert assumes circular orbits despite that the chaotic orbits and the short dynamical lifetime of Centaurs.

Now we try to combine the orbital evolution and thermal evolution. We calculate the orbital evolution of Centaurs and the crystalline fraction as functions of time. To calculate the crystalline fraction, we use equation (26) in Kouchi et.al. (1994) that gives the crystalline fraction of water ice under the temperature which varies with time. We calculate the temperature as a function of the heliocentric distance. We found that the crystallization timescale is much shorter than that of the propagation of the heat wave from the moment the object reaches a new surface thermal balance in the giant planets region, 10^4 -5 years, derived by Guilbert (2012). We also found that the orbital distribution obtained from observations is roughly well reproduced assuming Guilbert's timescale and our orbital integration. In the presentation, we will estimate and discuss the fraction of new Centaurs by comparing our results and the observations.

Keywords: Centaurs, orbital evolution, amorphous ice, cometary activity

Chemical composition diversity among impact-generated atmospheres on terrestrial planets: The effect of impact velocity

Hideharu Kuwahara^{1*}, Seiji Sugita¹

¹Complexity Sci. & Eng., Univ. of Tokyo

Prebiotic chemistry and climate conditions of early Earth and/or Mars would have been suitable for origin and evolution of life. The chemical composition of atmospheres during early evolution stages is important for understanding these factors.

Impact-generated atmospheres would occur on terrestrial planets immediately after their accretion and perhaps during the late heavy bombardment (LHB) period in the solar system. The approaches taken by previous studies on impact-generated atmospheres, however, may not have been accurate; they estimate the composition of impact-induced vapor with equilibrium calculation as a function of temperature under constant pressures [e.g., 1, 2]. This approach is appropriate if chemical reaction in impact-induced vapor is controlled by radiative cooling because radiative cooling decreases temperature while pressure is kept approximately constant. In reality, impact-induced vapor adiabatically expands; nevertheless such behaviors have not been considered. Entropy gain during the shock-compression phase controls the temperature-pressure pathway of the decompression phase. Thus, estimation of the initial entropy gain and subsequent quenching are the key for accurate estimation of the chemical composition of impact-generated atmospheres. The goal of this study is to model chemistry within adiabatically expanding impact-induced vapor, and investigate how sensitively impact-generated atmospheres depend on impact velocity.

Thermodynamically stable chemical compositions depend on temperature, pressure, and elemental compositions. Thus, constraints on these values are required for modeling chemical compositions of impact-generated terrestrial atmospheres. In this study, we assume CI chondrites as the impactor that mainly contributes volatiles to terrestrial planets during the heavy bombardment [e.g., 3]. To determine the temperature-pressure paths of adiabatically expanding vapor, we estimate the entropy gain during the shock-compression phase using the Hugoniot equation of state for silica [4]. Then, we calculate the major composition of a gas and condensed phase along isentropic lines within a range of pressures (0.01-10000 bars) and temperatures (500-2500 K). The model calculations are performed using a Gibbs free energy minimization code [5]. Elements included in our calculations are H, C, O, N, S, Mg, Al, Si, Fe. Elemental abundances used in our calculations are taken from [6].

Our calculation results show that the redox disproportionation of carbon occurs at low entropy states achieved by low-velocity impacts (<13km/s). For high-velocity impact (>17km/s), impact-induced vapor is rich in diatomic molecules, such as CO and H₂. For low-velocity impact-induced vapor (<13km/s), CH₄ becomes thermodynamically stable even at high quenching temperatures (>1000K). This is because the adiabatic curve for low entropy states undergoes higher pressures at a given temperature. High pressure is thermodynamically favorable for the formation of polyatomic molecules, such as CH₄ and NH₃; i.e., Le Chatelier's principle. These calculation results strongly suggest that the chemical compositions of impact-generated atmospheres among terrestrial planets may be different even if the composition of accreting material were same, suggesting that early Mars and early Earth may have possessed a CH₄-rich reducing atmosphere and a CO- and CO₂-rich more oxidizing atmosphere, respectively.

References: [1] Hashimoto G. L. et al. (2007) JGR, 112, E05010. [2] Schaefer L. and Fegley B. (2010) Icarus, 208, 438-448. [3] Alexander C. M. O' D. (2012) Science, 337, 721-723. [4] Kurosawa K. et al. (2012) Am. Inst. of Phys., 855-858. [5] Gordon S. and McBride B. J. (1994) NASA Reference Publication 1311. [6] Wasson J. T. and Kallemeyn G. W. (1988) Philos. Trans. R. Soc. London Ser. A, 325, 535-544.

Keywords: Impact, Atmospheric composition, terrestrial planets

Impact experiments on a granular layer: an implication for crater scaling laws and the artificial Hayabusa 2 SCI crater

Sayaka Tsujido^{1*}, Ayako Suzuki², Masahiko Arakawa¹, Minami Yasui³

¹Graduate School of Science, Kobe University, ²Center for Planetary Science, ³Organization of Advanced Science and Technology, Kobe University

Introduction : Regolith formation and surface evolution on asteroid are caused by high velocity impacts of small bodies. The ejecta velocity distribution is one of the most important physical properties related to the crater formation and it is necessary to reconstruct the planetary accretion process among planetesimals. The surface of small bodies in the solar system has a various property on the porosity, strength and density. Therefore, the impact experiment on the target with the various properties is necessary to clarify the crater formation process applicable to the small bodies in the solar system. These results obtained from the target with the wide range of condition could help us to speculate the physical properties of the asteroid surface from the artificial impact crater made by Hayabusa 2-SCI. We would try to determine the surface strength and the porosity by means of the observation of the ejecta shape and the velocity distribution.

Experimental method: The cratering experiment was made by using a vertical type one-stage light gas gun (V-LGG) set at Kobe Univ. We newly developed a special sabot-stopper system to exclude the disturbance of accelerating gas from the growing ejecta curtain. We used 4 types of targets: that is, they are the 100micron-glass beads target (porosity 37.6%), the 500 micron-glass beads target (porosity 37.6%), the 1~3mm granular pearlite (porosity 96.7%) and the crushed pearlite with the size of a few 100 microns (porosity 84.9-88.4%). These granular materials were put into the stainless steel container with the diameter of 30cm and the depth of 11cm. The target container was set in a large chamber with the air pressure less than 10^3 Pa or 10^5 Pa. The material of the projectile that we used was an iron, a zirconia, an alumina, a glass, and a nylon, and it had a diameter of 3mm (2r) and was launched at the impact velocity (v_i) of 25 to 217m/s.

We made an impact experiment using an alumina sphere projectile on the 500-micron granular target and observed each glass bead by using a high speed digital video camera (nac memrecam HX-3) taken at 10^4 FPS. Then, we measured the ejection velocity and the initial position of each bead. We successfully obtained the relationship between the initial ejection velocity and the initial position for the bead ejecta. We also made the impact experiments on the 100-micron glass beads target and the pearlite target using various type of the projectile at a constant velocity of 100 and 200 m/s, and observed the crater size and the shape of ejecta curtain, especially for the ejecta angle.

Result: We found that the ejecting velocity of the glass bead for the 500-micron target decreased with increasing the distance from the impact point. The obtained empirical equation between the ejection velocity and the initial position is as follows, $v_e/v_i=0.66(x_0/r_0)^{-1.6}$, where v_e is an ejection velocity of glass beads, x_0 is the initial position of ejecting beads. The ejection angle of the beads is found to be almost a constant of 40 degree irrespective of the initial position. The crater size for the 100-micron target increased with the projectile density at the constant impact velocity and it was analyzed by using a crater scaling law to derive an empirical parameter characterizing the granular target. The relationship between the normalized crater size and the impact condition was written by $[R*(\rho_t/m)^{(1/3)}]/[(\rho_t/\rho_p)^{0.03}]=1.9*[g/(v_i^2)]^{-0.17}$, where R is the radius of a final crater, ρ_t is the density of the target, ρ_p is the density of the projectile, m is the projectile mass, and g is the acceleration of gravity. From this obtained equation for the crater scaling law, we determined two key parameters of the coupling parameter ($C=r v_i^{\mu} \rho^{\nu}$): they are $\mu=0.40, \nu=0.36$. In the case of the crushed pearlite target, we found that the crater type changed from an incompressive type to a compressive type at the porosity from 83 to 88%.

Crater rays in impact experiments and numerical simulations

Toshihiko Kadono^{1*}, Ayako Suzuki², Koji Wada³, Satoru Yamamoto⁴, Masahiko Arakawa⁵, Seiji Sugita⁶, Akiko M. Nakamura⁵

¹University of Occupational and Environmental Health, ²Center of Planetary Science, ³Planetary Exploration Research Center, ⁴National Institute for Environmental Studies, ⁵Kobe University, ⁶University of Tokyo

Crater rays, which often adjoin the craters on the surfaces of the planets and satellites, appear also in laboratory impact experiments. Formation mechanism of such crater rays has been considered so far but not clear. Here, we carry out impact experiments with granular targets and observe the pattern formation in ejecta, taking consecutive images of ejecta by a high-speed camera, and final ray-patterns around craters. Also, we numerically investigate two-dimensional pattern formation process of granular materials using a discrete element method (DEM) simulation. Moreover, we analyze the crater rays on the surface of the Moon, using the satellite data of Kaguya.

Based these results, we find the characteristic features of the ray formation mechanism as,

1. Crater rays are not always straight in the radial direction; they complexly twine each other (intertwine).
2. Granular materials in the ejecta do not collide elastically each other during their flights.

We quantitatively compare the results of the experiments, numerical simulations, and satellite data analysis and investigate some scaling-laws about the relations between the ray patterns and the impact conditions such as the impactor size and velocity, the size of target granular particles, and gravity.

Keywords: crater ray

Effect of incident angle on crater dimensions with limestone targets

Ayako Suzuki^{1*}, Masato Kiuchi², Yasunari Komoto², Eri Matsumoto², Toshihiko Kadono³, Akiko Nakamura², Sunao Hasegawa⁴, Kosuke Kurosawa⁴, Masahiko Arakawa², Seiji Sugita⁵

¹CPS, Kobe Univ., ²Kobe Univ., ³Univ. Occupational and Environmental Health, ⁴ISAS / JAXA, ⁵Univ. Tokyo

Impact craters are common on the surface of solid bodies in our Solar system, and the majority of them are formed in oblique impacts. The effects of incident angle on impact cratering are important to derive scaling laws of impact craters and to understand the formation of secondary craters. However, there are not much experimental data of oblique impacts, especially in the strength regime. Recently, high-resolution images of the surface of planets and small-bodies allow us to see small craters in meters (e.g. McEwen et al., 2007). There are many terrestrial craters in the strength regime, such as the Carancas crater (e.g., Tancredi et al. 2009) and the Kamil crater (Folco et al. 2011). In this study, we performed impact experiments into sedimentary rock varying incident angle, to examine the effect of the angle on the crater dimensions.

Two-stage light gas gun placed in ISAS/JAXA was used. The projectiles were nylon spheres of 7 mm in diameter. The targets were blocks of limestone with 15 cm cube. The tensile strength, bulk density, and porosity of the limestone are 4.6 MPa, 2.24 g/cm³, and ~17%, respectively (Suzuki et al. 2012). The impact velocity is ~2.5 km/s, and the incident angle (theta; measured from the target surface) is varied as 5, 10, 20, 30, 45, 90° (vertical impact). The impacts are recorded by a high-speed digital video camera. After each shot, we measured the length (the maximum dimension of the crater along the projectile trajectory) and width (the maximum dimension perpendicular to the trajectory) with a digital caliper. We also made 'a digital topographic data' of the crater by means of a digital microscope (KEYENCE, VHX-1000), then obtained the crater volume and depth.

There is a pit in the center of the crater at the vertical impact (theta=90°), while no noticeable pits are observed in craters of theta < 45°. The ratios of lengths, widths, depths, and volumes against the values of vertical impacts are proportional to (sin theta)^{0.54 ± 0.01}, (sin theta)^{0.49 ± 0.01}, (sin theta)^{0.66 ± 0.02}, (sin theta)^{1.61 ± 0.09}, respectively. The power of the volume ratio (1.61 ± 0.09) is similar to those obtained by aluminum impacts into granite (Gault and Wedekind 1978; 1.80 ± 0.16). In the strength regime, it is known that the crater volumes are proportional to the impact energy (namely, to the square of the impact velocity). Our results are consistent with the concept that crater-scaling relations can adequately accommodate the impact-angle effects by using only the vertical velocity component (Gault and Wedekind 1978; Chapman and Mckinnon 1986).

The ratio between the length and width is constant of 1.11 ± 0.11 over the range of the incident angle from 90° to 5°, while the critical angle where the ratio deviate from unity is ~15° (Gault and Wedekind 1978) and ~5° (Burchell and Whitehorn 2003). One reason for this may be that the nylon projectile is easy to break and the top part of the projectile does not shear off (so-called 'impact decapitation' (e.g., Burchell and Whitehorn, 2003)). Without impact decapitation, the length of the crater decreases when theta decreases, in the same manner as the width decreases. However, the crater of 5° in incident angle has a raised part in the downstream side, suggesting it would be a spall fragment when it's tore off. In the strength regime, spall fragments play a big role in shaping craters. We need a number of shots to minimize the effects of spall fragments.

Averaged diameter is defined as the average of length and width of the crater. The crater depth normalized by the averaged diameter is constant of 0.16 ± 0.01 in the range of theta from 20° to 90°. The normalized depth at theta = 5° and 10° is smaller than the value. This trend is due to depths becoming small faster than lengths and widths, and would be because the density of the nylon projectile is about a half of that of limestone target and the projectile is difficult to penetrate the target.

Effect of surface layering on the apparent thermal inertia

akari yoshida^{1*}, Takenori Toyota¹, Kei Kurita¹

¹Earthquake Research Institute, The University of Tokyo

Thermal inertia is a key property controlling diurnal temperature variation at the surface of planets. It is defined as a function of thermal conductivity, heat capacity, and density, all of which depend primarily on the physical structure of the surface layer. Thermal inertia of Mars has been derived from Viking, Mars Global Surveyor and Mars Odyssey data. It tells us a structure of the surface layer. For example, low thermal inertia indicates extensive dust deposits and higher thermal inertia suggests combination of particle size, rock abundance and induration of soils.

An extremely low thermal inertia values such as 5-60 tiu and 24-60 tiu have been reported in the equatorial and middle latitudes from these observations. Since the thermal conductivity is the most sensitive to the particle size under martian atmospheric pressure, such a low thermal inertia indicates small grain size as low as 10 micron. But, these particles can be easily blown away by a strong wind on Mars and it is difficult for them to form a uniform layer on the structure. In this presentation we consider the possibility that a layered structure yields apparent low thermal inertia.

To demonstrate possible effect of the layering we conducted laboratory experiments. We utilized the structure having an acrylic plate on top of a polystyrene form block or vesiculated particle layer. They are heated periodically by an infrared lamp from above. Using the infrared thermometer and thermocouples, we measured the temperature at the surface, bottom of the acrylic plate and inside the lower Polystyrene form and the granular layer.

Thermal relaxation time of this layered systems is the most fundamental factor here, which represents the time that the amplitude of temperature inside the material becomes 1/e compared with the surface.

We estimated the thermal inertia from experimental data. It is found that the thermal inertia is lower than the value calculated from the physical properties when the given period is longer than the thermal relaxation time of the surface layer. It is because the material behaves infinite body when the period is shorter than the thermal relaxation time.

On the other hand it behaves as a finite body if the period is longer than the relaxation time. In this situation the temperature at the bottom of the surface acrylic plate becomes high because of lower thermal conductivity of the lower layer. This means the thermal gradient becomes lower and the heat flux to the interior seems small, which results in apparently low thermal inertia

In our experiments we can demonstrate a simple layered structure; a thin layer having higher thermal conductivity on top of a layer with low thermal conductivity can produce apparently low thermal inertia. In the martian remote sensing diurnal temperature variation is used to infer the thermal inertia, which measures the value of the surface within the thermal penetration depth of several to 10 cm. If the layered structure exists in this range having lower conductivity of the lower layer.

We discuss several geological processes to produce layered structure on Mars.

Keywords: thermal inertia, geological structure, thermal relaxation time

Effects of the temperature dependences and surface roughness of the asteroid 1999JU3 on the surface temperature mapping

Jun Takita^{1*}, Satoshi Tanaka², Hiroki Senshu³, Tatsuaki Okada²

¹Graduate school of science, Tokyo university, ²Institute of Space and Astronautical Science, JAXA, ³Planetary Exploration Research Center, Chiba Institute of Technology

The observational program with thermal infrared imager to detect its target asteroid 1999JU3 and the strategies to estimate the surface physical state with obtained data are now under constructed in Hayabusa 2 mission. It is necessary to clear and understand the mechanism to realize the observed space-resolved data of surface temperature. We consider the temperature dependence of surface material plays important role in surface temperature of airless small bodies, especially NEA asteroids which maximum and minimum temperature differ significantly. In addition to this, we are now investigating the effect of the surface roughness on surface temperature distribution of asteroids and comets. The beaming parameter which has close relationship with surface roughness is necessary for the explaining the ground based spatially-none-resolved surface brightness and temperature of asteroids. Recent DEEP-IMPACT or EPOXI missions have revealed that the shape model alone could not be enough to reproduce the observed surface temperature distributions but it would be possible with the help of the effect of surface roughness in some appropriate ways. The surface roughness would also generate the interactive heating effect through radiative energy exchanges between its and adjacent surfaces.

We took six orbital elements into account to calculate the planetary position of the asteroid as well as the orientation of the spin axis so as to simulate the distance from the sun and the incident angle of solar energy into the surface. The shape of the numerical model is set to be spherical and subject to one dimensional heat conduction equation in none steady state. We have made the temperature mapping of the target asteroid to use this model. The distribution of thermal properties of heat conduction medium is constant toward inner direction, which has temperature dependencies except for the density. We applied the experimental result of temperature dependencies of lunar samples to this model. The numerical calculation showed that the difference of surface maximum temperature in one rotation near perihelion was about 10K between temperature dependent and none-dependent models. Thus we thought this effect would not be negligible to derive the thermal inertia of the asteroid with TIR instrument. We have now been performing the estimation of the effect of surface roughness on the surface temperature to construct some simple models. We will present the result of this effect on this meeting.

It is important to distinguish the geometric effects from the thermo physical effects to estimate the physical state of the planetary surface. This is not only indispensable with the determination of sampling rate of TIR thermal images but also practical in SCI impact experiments in terms of finding the locations of impacting center and the smashed debris.

Keywords: Hayabusa2, thermal infrared imager, thermal inertia, temperature dependence, roughness, equation of heat conduction

Thermal conductivity measurements of sintered powder under vacuum condition

Shoko Tsuda^{1*}, Kazunori Ogawa¹, Naoya Sakatani¹, Yu-ichi Iijima¹, Rie Honda², Satoshi Tanaka¹

¹Institute of Space and Astronautical Science, ²Kochi University

In the planetary formation process, powder like dusts would have formed into planetesimals that have grown into proto-planets or asteroids through collisions between each other. Although efficiency of collisional accretion depends on physical properties (such as density and strength), their change due to thermal metamorphism has not been fully understood. Some planetesimals might have served as parent bodies of meteorites, and evidence of their thermal metamorphisms could give us information of size and formation time of the planetesimals. Therefore, it is important to investigate their thermal evolution and resultant change in the physical properties.

Thermal conductivity of the planetesimal constituents is one of the important parameters for examination of the thermal evolution. While the thermal conductivity of typical rocks is about 1 W/mK, that of powder is in the order of 0.001 W/mK under vacuum, which is lower than the value of rocks by three orders of magnitude. Because of thermal insulation by the powdered materials, even small planetesimals with the radius as small as 10km might have experienced temperature more than 1000 K (Ogawa, 2013), so that sinter bonding might have formed between powder particles that could have caused a significant change of the thermal conductivity.

Henke et al. (2012) calculated the thermal evolution of primitive porous planetesimals consisted of powdered materials as a model of parent bodies of chondrites. They assumed that sintering occurred as the internal temperature increased, which process made planetesimals thermal conductivity higher by one to two orders of magnitude. Measured data of thermal conductivity of some kind of powders under vacuum is available (e.g. Sakatani et al., 2012), but there are few reports, in which the thermal conductivity of sintered material is measured. In their study, they used thermal conductivity derived as a function of porosity based on the measured value of silicate powder and chondrites.

However, based on our measurements of the thermal conductivity of glass beads (Sakatani et al., 2012), a positive correlation between the thermal conductivity and the pressure (thus, the inter-particle contact area) was observed. Therefore, the thermal conductivity should be re-examined as a function of the contact area instead of porosity.

In this study, we aim at investigating thermal conductivity of the sintered materials under vacuum condition, in order to provide constraints on the thermal conductivity of the sintered materials in planetesimals. Glass beads of several particle sizes were used as pre-sintered powder samples.

For sample preparation, we examined neck radius variation due to the heating temperature and the heating duration using a theoretical expression (Sirono, 1999; Poppe, 2003). The results indicated that, in order to make the neck radius 10 times larger than that is formed by heating for 0.1 hours, increasing heating time to 1000 hours are equivalent with increasing heating temperature by 100 K. Thus we adopted change the heating temperature instead of heating duration to control the sintering contact area.

Currently we are planning to measure the thermal conductivity of sintered samples by so-called line heat source method. Two methods are considered for installation of a heat system in the samples: (1) putting the system in the glass beads and then heating both samples and the system to induce sintering of glass beads and (2) putting the system between two separate sintered samples created under the same condition. In the former case, heating during sintering may induce the change of electric resistance of the heating wire by oxidation and melting of a resin used between the wire and the thermocouple. The latter case is free from these problems, thus we adopted the latter method for installation of the line heat source system. We present detailed explanation of the measuring method and results of these experiments in the presentation.

Keywords: sintering, powdered materials, thermal conductivity

Early thermal evolution of planetesimals considering low thermal conductivity of powdered materials

Maho Ogawa¹, Naoya Sakatani^{1*}, Yu-ichi Iijima¹, Kazunori Ogawa¹, Shoko Tsuda¹, Rie Honda², Masahiko Hayakawa¹

¹Institute of Space and Astronautical Science, ²Kochi University

Dust materials in protoplanetary disk accumulated into planetesimals. Protoplanets and asteroids have been considered to be formed by the collisions between the planetesimals. Efficiency of the collisional growth depends on physical properties and internal structure of the bodies. Therefore, it is important to consider the evolution of the physical properties and internal structure of the planetesimals due to thermal metamorphism. In previous studies, the thermal evolution of meteorites parent bodies were calculated in combination with metamorphic temperature or cooling rate estimated from the meteoritic analysis. However, most of these studies used the physical properties, such as thermal conductivity and density, of the meteorites as initial parameters of the parent body. Since the planetesimals accumulated from the dusts are considered to be porous bodies consisted of powdered materials, the above assumption would be improper. The initial properties of the planetesimals are important parameters controlling the thermal evolution and the resultant change of the internal structure. Among these initial properties, we focused on the thermal conductivity.

It is known that the powdered materials have low thermal conductivity compared with rocks having the same composition. Especially under vacuum environment, silicate powders have extremely low thermal conductivity about 0.001 W/mK. Therefore, if assuming the porous body consisted of powdered materials as the initial structure of the planetesimal, the subsequent thermal evolution would be different significantly from the previous models that assumed the physical properties of the meteorites. In this study, we aimed at investigating the effect of the powdered materials of low thermal conductivity on the thermal evolution of the planetesimals.

We numerically solved the equation of one-dimensional and spherically symmetric heat conduction, with the thermal conductivity, porosity, and formation time and size of the planetesimal as variable parameters. For the thermal conductivity of the powdered materials, which is the most interesting parameter in this study, we used experimental values we measured for glass beads (porosity of 40%) under vacuum. Since the thermal conductivity of the powdered materials depends on the cube of the temperature, it varies significantly during the thermal evolution. The temperature dependence was also included in our model.

We found that even planetesimals as small as 10 km in radius experience the significant heating above 2000 K at the center (see figure). Previously, it has been considered that the radius of the planetesimal about 100 km is required in order to heat up sufficiently to form the thermally metamorphic meteorites. Our calculation indicates that the planetesimals smaller than 10 km can serve as the parent bodies of chondritic and/or differentiated meteorites.

When comparing the temperature evolution between the models including and excluding the temperature dependence of the conductivity, the former had lower peak temperature by about 500 K than latter. While the temperature was maintained around the peak temperature for more than 100 m.y. for the latter case, for the former case the temperature dropped to a half of the peak temperature after 20 m.y. Therefore, the temperature dependence of the thermal conductivity of the powdered materials should be included in the model calculation.

When the temperature increases, the powdered materials will be sintered at a certain temperature. Because the thermal conductivity of the sintered materials will be higher than the not-sintered powdered materials, the sintering affects the subsequent thermal evolution. Furthermore, the change of the physical properties after the sintering would be important for the collisional growth between the planetesimals. In this presentation, we will also present the calculation results that include the effect of the sintering.

Keywords: powdered materials, planetesimal, thermal evolution

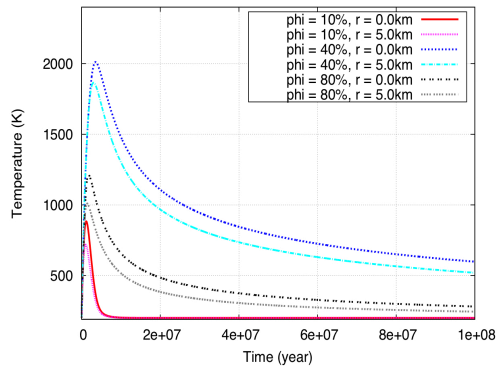


Figure: Thermal evolution of planetesimals of 10 km radius formed at 2 m.y. after CAI formation. "phi" and "r" in the legend refer to the porosity and distance from the center, respectively.

Experimental study on the impact strength of planetary bodies damaged by multiple collision

Ryo Hayama¹, Masahiko Arakawa^{1*}, Minami Yasui², Yuri Shimaki³

¹Graduate School of Science, Kobe University, ²Organization of Advanced Science and Technology, Kobe University, ³Graduate School of Environmental Studies, Nagoya University

High velocity collisional disruption of small icy bodies is one of the most important physical process related to the formation of the debris disk and the collisional growth of planetesimals in the outer solar nebula. Therefore, there are a lot of studies on the collisional disruption of icy bodies such as polycrystalline ice and snow systematically. As a result, the impact strength of polycrystalline ice was obtained to be 90 J/kg, and the snow was found to change the impact strength with the porosity. While in the case of the collisions among the real small bodies, the bodies could be sometimes collided at many times before they were disrupted. We definitely observe so many craters on the surfaces of icy bodies and the large crater that is more than a half of the size is also observed in many icy bodies. Thus, we should consider the effect of these pre-impact damages in the icy bodies when we apply our laboratory results to the real collisions in the solar system. Because these pre-impacted bodies could be weaker than the intact bodies. Therefore, we studied the effect of pre-impact damage on the impact strength of polycrystalline ice systematically, and the effects of the pre-impact time and the each impact energy on the impact strength was determined quantitatively.

Impact experiments were made by using a vertical gas gun set in a large cold room which room temperature was -15 degree or -10 degree. The ice target was a cube with the size from 3 to 10 cm ($M_t=100 - 3000$ g) and the projectile was a icy cylinder with the size of 1.5cm or 1cm ($m_p=1.5$ g or 0.2g). The impact velocity was from 100 to 480 m/s, and the projectile was collided on the different surface of the cube target or the same surface for the multiple impact experiment. We also change the energy density given to the target for each impact. After the impact, the target was recovered to measure the weight of each fragment. When the target was not disrupted severely, the elastic velocity through the recovered target was measured at 3 different positions. We also measured the static indentation strength of the recovered target, so the target was sliced into 3 plates and there plates were slowly pushed by an indenter. The elastic wave velocity of each plate was measured before the indentation test. Then, we tried to obtain the relationship between the elastic wave velocity and the indentation strength.

In the case of the impact at the different surface of the cube target, we found that the sum of the energy density for each impact (Q_{sum}) was a good parameter to describe the impact strength because the relationship between Q_{sum} and the largest fragment mass consists each other irrespective of the impact time and they are consistent with the result of the intact ice disrupted at once. In the case of the impact at the same surface, the Q_{sum} was apparently larger than that was necessary for the impact at the different surface. This difference of the impact strength depending on the impact surface could be caused by the difference of the internal crack density and the distribution. Then, we studied the relationship between the elastic wave velocity and the indentation strength, and we obtained the following empirical equation, $Y/Y_0=1-1.34 dV/V^{0.78}$. We applied this equation to the scaling parameter P_I proposed by Mizutani et al. (1990) and studied the relationship between P_I and the largest fragment mass. Thus, we found that all the data merged on one line and the empirical relationship was obtained to be $m_l/M_t=0.0413P_I^{-4.82}$. So, the effect of the pre-impact damage by multiple impacts is found to be quantified by the elastic velocity. This enable us to estimate the impact strength of the real small icy bodies by the measurement of the elastic wave velocity of these interiors.

Keywords: icy planetesimals, impact disruption, crack, sound velocity, mechanical strength, scaling law

Dynamic compaction experiments of snow: Implications for low-velocity impact compaction of icy pre-planetesimals

Minami Yasui^{1*}, Kana Sakamoto², Masahiko Arakawa³

¹Organization of Advanced Science and Technology, Kobe University, ²Faculty of Science, Kobe University, ³Graduate School of Science, Kobe University

Introduction: In the standard solar model, planetesimals could form by gravitational instability in the dust layer of a proto-planetary disk. However, there is a significant problem that planetesimal could not grow because of dust settling disturbance by turbulent flow in the disk. We focused on a pre-planetesimal, which is a body with the diameter of cm to several hundreds meters. Recently, some researchers suggest that planetesimals could form by impact coagulation of pre-planetesimals. However, there are also some problems, such as catastrophic disruption. Some researchers studied the formation processes of pre-planetesimals by numerical simulations. Geretschauser et al. (2011) proposed the impact model of porous silicate-dust aggregates, and found seven impact regimes (compaction, disruption, and adhesion) depending impact velocity and size ratio of impactor and target, and the compaction degree was different with regime. However, this model did not include compaction curves measured in laboratory experiments. In this study, we conducted low-velocity impact experiments for high porous snow simulating icy pre-planetesimals, and studied the impact compaction conditions. We measured the density profile changing with depth, compaction area size, and stress, and obtained the empirical equations related to density distribution and compaction area.

Experimental methods: We did impact experiments in the cold room at -10 degree C in ILTS, Hokkaido University. The projectile was a stainless cylinder with the diameter of 25 mm, the height of 40 mm, and the mass of 149 g. On the lower, a PVC disk with the diameter of 26 mm was set due to suppress the ejecta. The projectile was accelerated by free fall, and the drop distance changed from 50 to 900 mm. The impact velocities were 0.7 to 3.5 m/s. The target was prepared by packing ice grains into the acrylic tube with the diameter of 26 mm. The porosities were 70, 80, and 90 %. Ice grains were made by spraying water into LN₂, and then the ice grains were sieved to sort grains from 50 to 500 micron-m. The target has the length of 100 mm, and the blue ice grains were put into the target every 20 mm from the bottom due to measure the density changing with depth. The blue ice grains were produced by spraying blue water into LN₂. The impact compaction of the target was observed by a high-speed digital camera. The shutter speed was set to be 20 and 50 micron-s, and the frame rate was set to be 3000 and 5000 fps. The acceleration sensor was set on the upper surface of projectile to measure the stress. The voltage measured by acceleration sensor was recorded by oscilloscope and data logger. The sampling number of data logger was set from 2.5×10^5 to 10^6 and the sampling interval was set to be 20 micron-s.

Results: We analyzed the stress by using the data of acceleration sensor and high-speed camera images. The maximum stress, s_{max} , which is defined to be a maximum stress on the stress profile, was 20-100 Pa for 70 % snow, and 15-50 Pa for 80 % snow, and that of 70 % snow was 1.3-2 times larger than that of 80 % snow. Additionally, the s_{max} increased with the impact velocity in both targets. The stress obtained from the data of acceleration sensor corresponded to that for high-speed camera images. Furthermore, the yield strength, Y , calculated by Kinoshita method and these obtained stresses were almost same. Next, we compared the final density of uppermost layer of target, r_1 , and the s_{max} to study the density profile. As a result, the r_1 increased with the s_{max} , the relationships between r_1 and s_{max} were expressed as $r_1 = 1.7 \times 10^2 s_{max}^{0.2}$ for 70 % snow and $r_1 = 1.2 \times 10^2 s_{max}^{0.3}$ for 80 % snow, respectively. Finally, we calculated the bulk modulus, K , by using the relationship between the yield strength, Y , and the average density of target, r_{ave} , and the K was 1.8 MPa for 70 % snow and 0.2 MPa for 80 % snow, respectively.

Keywords: icy pre-planetesimal, impact compaction, low-velocity impact experiment, density profile, compaction area, bulk modulus

Evolution of planets with oceans within the Water World Regime around a main sequence star

Satoshi Fukushima^{1*}, Shintaro Kadoya¹, Eiichi Tajika²

¹Department of Earth and Planetary Science, The University of Tokyo, ²Department of Complexity Science and Engineering, The University of Tokyo

The Habitable Zone (HZ) around a main sequence star is the orbital condition in which planets could have liquid water on their surface, although greenhouse effect of the atmospheres due to some greenhouse gasses (e.g., CO₂) is generally required. On the other hand, we propose here the Water World Regime (WWR) which is the orbital condition for the planets to have liquid water even if the planetary atmospheres do not have any greenhouse gasses except water vapor. The WWR is therefore much narrower condition than the HZ, estimated to be an annual mean insolation from 1.07 to 1.41 S₀ (where S₀ is the solar constant for the present Earth). Most of the WWR condition is, however, under the moist greenhouse condition in which water should escape to space during the planetary evolution (e.g., Kasting, 1988). The time scale of water loss should therefore be discussed for the planets with different amount of H₂O and XUV from the central stars.

We estimated life time of oceans on the planets orbiting within WWR by assuming water loss due to hydrogen escape by diffusion-limited (Hunten, 1973 ; Walker, 1977), and energy-limited water loss mechanisms (Watson et al., 1981), with considering stellar luminosity evolution (Gough, 1981 ; Iben, 1967), and stellar EUV evolution (Lammer et al., 2009).

We will show that the life time of oceans may be longer than that considered generally. For example, if the Earth is orbiting within the WWR around a M-type star and has liquid water of 5 times the amount of ocean today, liquid water may be able to exist for 10 billion years.

Keywords: Extrasolar planet

Climate evolution of extrasolar terrestrial planets with water and carbonate-silicate geochemical cycle

Shintaro Kadoya^{1*}, Eiichi Tajika²

¹The University of Tokyo, ²The University of Tokyo

The surface environment of a habitable planet has been constrained in terms of orbital semi-major axis and an effective solar flux, focusing on the existence of liquid water, that is, the habitable zone (HZ) around main sequence stars (e.g., Kasting et al., 1993). It has been also pointed out that the carbonate-silicate geochemical cycle would be essential for maintaining the climate of a habitable planet (e.g., Tajika, 2003). However, the whole picture of evolution of climate of planets with carbonate-silicate geochemical cycle has not been known.

In this study, we investigate the climate evolution of an Earth-like planet (actually, the Earth itself) around a G-type star (= Sun). Steady states of climate of Earth-like planets are estimated systematically with a simple climate model coupled with a carbonate-silicate geochemical cycle model. We classified climates of Earth-like planets within the HZ into three modes, in terms of stabilizing mechanism. Then, the climate evolution is estimated based on the steady state solutions of the climate with models of the stellar evolution and the thermal evolution of planetary interiors. The results indicate that, on an Earth-like planet (the size of the Earth) orbiting around a G-Type star, climate depends on the thermal history of the planet in the early stages of its lifetime, and then depends on the stellar evolution. The climate evolutions are also estimated for the different mass both for stars and planets.

Keywords: Extrasolar planetary system, Habitable zone, Habitable planet, Carbonate-silicate geochemical cycle, EBM

Local N-body Simulation for Accretion of Particles onto Moonlets in Saturn's Rings

Yuki Yasui^{1*}, Keiji Ohtsuki², Hiroshi Daisaka³

¹Dept. Earth Planet. Sci., Kobe Univ., ²Dept. Earth Planet. Sci., Kobe Univ./CPS, ³Hitotsubashi Univ.

Gravitational accretion of particles in circumplanetary disks is an important issue related to the origin of ring-satellite systems of giant planets in the Solar System. Observations by the Cassini spacecraft indicate that the small satellites within the orbit of Pandora orbiting just outside Saturn's F ring were formed by accretion of small porous ring particles. N-body simulations demonstrated that a Hill sphere-filling body is produced by accretion of small porous particles onto a larger dense core. Propeller-shaped structures, which are produced by unseen embedded moonlets, have also been found in Cassini images of Saturn's A ring. Some of these moonlets may have formed by accretion of small low-density ring particles onto larger dense fragments. Thus, accretion in the rings may also be related to the origin of these embedded moonlets.

The criteria for gravitational accretion of particles in the Roche zone was derived based on the Hill approximation in the three-body problem. The criteria, which we call the "three-body capture criteria", state that colliding particles can become gravitationally bound if they are within their mutual Hill radius and E becomes negative value after inelastic collisions, where E is the sum of the relative kinetic energy and tidal potential energy of colliding particles. Furthermore, using the criteria, capture probability for collisions between ring particles was obtained by three-body orbital integration. However, many-body effects, which are not included in three-body calculations, are expected to become important as accretion of particles proceeds and aggregates are formed.

In our local N-body simulation, a moonlet is fixed at the center of the rectangular simulation cell. For each time step, particles not yet perturbed by the moonlet are added to the cell from the azimuthal boundaries. Particles leaving the simulation cell through the azimuthal boundaries are removed from the cell, but we retain the periodic boundary condition in the radial direction. In order to examine the accretion process and timescale for the growth of the moonlet in detail, we count the number of particles that form an aggregate by two different methods. First, we use the above three-body capture criteria for the moonlet and each of the colliding particles, and examine if a particle is gravitationally bound within the Hill sphere of the moonlet. However, in this method, the self-gravity of the particles accreted by the moonlet is neglected, and we underestimate the number of particles in the aggregate, because the number of particles accreted onto the moonlet increases with time. Second, in order to correct the above problem, we count the number of particles touching the aggregate as a member of the aggregate; we call this the "aggregate criterion".

Using the aggregate criterion, we calculate the accretion rate as a function of time, for calculations at the distance from Saturn that corresponds to $R_p=0.7$, where R_p is the ratio of the sum of radii of colliding particles to the Hill sphere radius. The accretion rate obtained by the N-body simulation agrees well with that obtained by the three-body calculation at the initial stage of accretion. As accretion of particles proceeds, the result of N-body simulation is slightly larger than the three-body results, because a significant number of particles have accreted onto the moonlet by this time, and the collision cross section of the aggregate is increased. After that, the aggregate reaches a quasi-steady state with a nearly constant number of constituent particles. Then, the aggregate repeats accretion and releasing of particles again and again. We also calculate the number of particles in the aggregate using the two different methods. We find that the three-body capture criteria underestimate the number of particles in the aggregate. The result obtained from the aggregate criterion also shows recurrent accretion and release of particles in the quasi-steady state.

Keywords: accretion, moonlet, Saturn's rings, N-body simulation

Inelastic Collisions between Icy Bodies: Dependence on Impact Velocity and Its Fluctuations

Koji Uenishi^{1*}, YANO, Ryosuke², Tatsuya Yoshida¹, Keisho Yamagami¹, SUZUKI, Kojiro²

¹Dept Aero/Astronautics, Univ Tokyo, ²Dept Adv Energy, Univ Tokyo

In a ring system, energy loss during collisions of particles may play a crucial role in determining not only the mean free path between collisions but also the physical characteristics of the ring (e.g., kinematic viscosity, spreading rate, thickness, shape) and the rate of cooling in the system. The coefficient of restitution is a key parameter for evaluating such energy loss during collisions (Dilley and Crawford, 1996). Icy particles are commonly found in the rings of Saturn, and due to their closeness to our living environment, their coefficient of restitution has been intensively studied. Earlier works on collisions of icy bodies normally suggest that the restitution coefficient strongly depends on the impact velocity. More recent approach to the problems of energy loss and cooling in a ring system includes the concepts developed in the theory of granular flow, but due to the lack of precise information about the velocity dependence of the restitution coefficient, it is often assumed that the coefficient is constant (velocity-independent) in granular flow-based analyses of inelastic collisions. Here, in order to better understand the physical characteristics of ice as a granular material and gain more quantitative information about the effect of impact velocity on the collisions of icy bodies, first, we experimentally monitor the mechanical behavior of an ice sphere impinging upon a plate of ice (235 mm x 320 mm x 60 mm) with a digital high-speed video camera system introduced in our laboratory. The diameter of an ice sphere is either 25 mm or 50 mm, and each sphere is kept in a freezer at a temperature of -10 degrees Celsius for more than 30 hours before every experiment starts. We intend to obtain the variation of the normal restitution coefficient for the free fall of spheres with 17 different falling distances between 40 and 450 mm. For that purpose, we take full-color digital photographs at a frame rate of 7,000 frames per second and record the collision process: From the photographs, we can calculate the velocities of an ice sphere just before and after the collision and with these velocities we may evaluate the normal restitution coefficient. We perform our preliminary series of experiments on collisions of ice spheres at least 10 times for each sphere size and falling distance at room temperature of 21 degrees Celsius. The range of falling distance mentioned above gives an impact velocity of 60-370 cm/s for 25 mm diameter spheres and 90-380 cm/s for 50 mm diameter ones. Care is taken not to induce any rotation and fracture of the ice spheres during the collision process. We also observe the roughness of the sphere surfaces as well as the fluctuations of the obtained coefficient for each sphere size and impact velocity. Then, based on the ED (Event-Driven) method, we perform numerical simulations of the cooling process during collisions of 3,000 ice spheres that are initially located randomly in a two-dimensional square. In the simulations, the experimentally obtained velocity-dependent restitution coefficient and its fluctuations are taken into account for the inelastic collisions between ice spheres. The results show the final temperature is about 4 % lower than that obtained without considering the fluctuations of the velocity dependence of the coefficient.

Keywords: ring system, icy bodies, inelastic collision, coefficient of restitution, cooling process, granular flow

Development of a simplified 3D shape measurement system for micro spherical object: application to chondrules

Keisuke Nishida^{1*}, Ayaka Tsuda¹, Eiichi Takahashi¹, Taishi Nakamoto¹

¹Earth and Planetary Sciences, Tokyo Institute of Technology

We developed a simplified system to measure the 3D shape of micro spherical object such as chondrules. This system consists of macro photography lens, consumer digital camera, and automatic mechanical stages and has a capacity to shoot pictures at up to 0.85 um/pixel. The camera and stages are automatically controlled by PC. Photographic images of a sample were obtained every 2 degrees up to 180 degrees in backlight to enhance the contrast between sample and environment for ease of binarization in image processing. The images were binarized and extracted coordinates of the outline of the sample in every degree to construct the 3D shape of the sample by our own software. The 3D shape can be exported as STL file, which is very common file format for 3DCAD and CG software.

In this study, we report the measuring results of 3D shape of chondrules separated from Allende CV3 chondrite (Tsuda et al, JPGU 2013).

Keywords: 3D shape, chondrule, Allende CV3 chondrite, spherical micro object

Chondrule Formation by Planetesimal Bow Shocks

Fumika Yamazaki^{1*}, Taishi Nakamoto¹

¹Tokyo Institute of Technology

Chondrules are mm-sized silicate particles included in most meteorites. Though it is known from experiments and observations that they experienced flash heating and melting in the solar nebula, the heating mechanism is still unknown. To comprehend chondrule formation may lead to understanding the environment in the solar nebula and the solar system formation.

One of the ideas for heating mechanism is the shock wave heating model. The model explains that, when the precursor dust grains run into the shock, they experience the gas drag heating, and dust temperature exceeds the melting point (e.g., Hood & Horanyi, 1991; Iida et al., 2001). In this study, we conduct detailed examination of dust heating by planetesimal bow shocks, which are the shocks occurring around eccentric planetesimals.

We carry out the calculation of 2-D grain trajectory and thermal history in the flow around the planetesimal taking account of melting and evaporation of the grains, which was not included in 2-D calculations of previous studies about planetesimal bow shock model (e.g., Nakajima, 2010, master thesis; Morris et al., 2012). Moreover, for detailed examination, we use the gas flow which is obtained by 2-D hydrodynamics simulations with H₂ dissociation and recombination as the background of grain motion.

Our results show that the grains avoid collision with the planetesimal thanks to the evaporation in some cases, and it affects the chondrule formation efficiency and the resultant size of heated grains. Using our calculations, the size distribution of chondrules and compound chondrule formation could be investigated and compared with the observations. We also show the chondrule formation condition by calculations with various nebula gas density and relative velocity of planetesimal to gas. Our results support the expectation that the solar nebula was more massive than MMSN model and that chondrules were formed in inner region of 3AU from the Sun.

Keywords: chondrule, bow shock, planetesimal, solar system formation, hydrodynamics simulations

Dust accumulation caused by thermal interaction between gas and dust in gas shock regions

Keisuke Watanabe^{1*}, Taishi Nakamoto¹

¹Tokyo institute of technology

Meteorites are important clues to investigate the environment of the early solar system. Chondrules are 0.1mm ? 1mm sized spherical igneous structure which are abundantly found in chondritic meteorites. Chondrule precursor dust grains once experienced melting caused by certain heating event, then recrystallized and formed their spherical form. Experimental constrains suggest that heating event was intense, heating duration is of the order of a few minutes and these events continued intermittently about three million years. This heating process was surely dominant in the early solar system but details are still unknown.

The most promising heating source for chondrule formation is gas shock wave heating in the protoplanetary disk. Previous works showed that gas shock waves can heat up the precursor dust grain temperature above melting point due to frictional heating. Iida et al. (2001) also showed that the gas temperature is higher than the dust temperature when the dust stops in the gas and its temperature attains maximum. In such a situation, the dust acts as coolant for the gas.

The gas in a relatively high dust density region is preferentially subjected to cooling by the dust. This preferential cooling makes the gas pressure minimum. Then the gas flows into the region because of the gas pressure gradient. This flow drags the dust into the high dust density region and it leads to further dust density enhancement. This one way thermal instability process may cause dust accumulation. Previous works concerning the gas shock wave heating model did not consider this process at all.

Here we investigate the possibility of dust accumulation by gas dust thermal interaction. To this aim we consider a gas dust two component fluid. We carry out one dimensional numerical calculation which includes both momentum and energy interaction between the gas and dust.

In our model, the gas loses energy via thermal collision with the dust due to the gas dust temperature difference. The dust gains energy from the gas and emits energy to outside of the system by radiation. Only the dust absorbs radiation from surrounding radiation field. The dust receives gas drag force and the gas receives back reaction. Only the gas feels self pressure gradient.

As initial condition we assume that there is a dust density maximum in the gas. We add dust density profile with Gaussian form on uniformly distributed dust density. The gas density is constant. The dust to gas mass ratio is unity at the maximum of the dust density, and one percent at far from the dust density maximum. We adopt typical gas and dust temperature, which are plausible after dust heating by gas shock waves. The gas temperature is higher than the dust temperature. The gas and dust velocity is assumed to be zero at first. From this initial setting we evaluate time evolution of the system.

We find that the gas in high dust density region cools faster than the gas in low dust density region. This difference of the cooling time scale of the gas makes pressure gradient of the gas. The gas begins to flow into the low gas pressure region and the gas density increases in the region. Drag force induces the dust inflow and the dust density also increases there. Gas and dust density enhancement lasts until the minimum gas temperature attains the temperature of the surrounding radiation field and decreasing of minimum gas temperature stops. In our setting, we show that the maximum gas and dust density increase is around five times larger than the initial density.

The gas density increases as to the system becomes isobaric. Isobaric condition shows that the gas density enhancement is several times larger than the initial gas density. Drag force can enhance the dust density as the same order of the gas density increase.

Future work is to investigate the consequence of this dust density enhancement.

Keywords: protoplanetary disks, chondrule, shock wave heating, dust accumulation, thermal instability

Radial Accumulation of Dust Boulders at a Boundary between Super/Sub-Keplerian Flow in a Protoplanetary Disk

Tetsuo Taki^{1*}, FUJIMOTO, Masaki², IDA, Shigeru¹

¹Tokyo Institute of Technology, ²JAXA

In the process of planetesimal formation, spiral-in of dust particles toward the host star is the most serious difficulty. One of the mechanisms to halt the spiral-in is a radial pressure bump in the disk, at which the boundary between local super/sub-Keplerian flow exists. However, according to accumulation of dust particles at the super/sub-Keplerian transition point, the dust frictional force alters the gas density profile (e.g., Kato et al., 2012).

We think that accumulation processes of the dust particles at the pressure bump, which has the similar size with the bump presented by Kato et al. (2009, 2010). We have investigated the time evolution of dust density distributions due to drag force from the protoplanetary disk gas, taking into account backreaction from the

dust particles to the gas consistently with local 1-D and 2-D hybrid simulations. We treat the disk gas as a grid-hydrodynamics and the dust particles as super-particles.

In 1-D simulations, we found that the gas density distribution is seriously deformed as the dust accumulates at pressure bump in the case with backreaction. At once, the dust density distribution is radially expanded around the boundary between super/sub-Keplerian flow. Finally, the dust particles resume the inward drifts,

and their density distribution achieves the gradual peak in the radial direction. Then the maximum dust-to-gas density ratio is unity.

In 2-D simulations, we confirm the driving of streaming instability in the dust dense region formed by the radial pressure bump. Due to the effect of streaming instability turbulence, the maximum dust-to-gas density ratio raises to 5, which is larger than 1-D results. However it is lower than the result of the 2-D or 3-D MHD simulations presented by Kato et al. (2012), which include the effect of inhomogeneous MRI turbulence.

These dust-to-gas density ratios is too small to drive the gravitational instability, which forms the planetesimals quickly, and the pressure bump is not able to maintain the halting of the dust particles. Therefore, we conclude that the halting mechanism of pressure bump is not able to form the planetesimals very well by itself. Then we suggest the possibility that the effect of the maintenance or restoration to the pressure bump might increase the dust density and form the planetesimals via gravitational instability.

Keywords: planetesimal formation, protoplanetary disk

Dynamics of charged dust particles in the magnetic field related to the dust infall problem in protoplanetary disks

Kenichiro Hirai^{1*}, Yuto Katoh¹, Naoki Terada¹

¹Department of Geophysics, Graduate School of Science, Tohoku University

In Protoplanetary disks, the velocity difference occurs between the rotational speed of gas and dust particles due to the pressure gradient of the disk gas. Since the motion of dust particles is affected by the headwind of gas, dust particles lose angular momentum and eventually fall into a central star. However, since in the region close to the central star we can expect a finite magnitude of the intrinsic magnetic field and a high ionization rate due to the strong radiation from the central star, the effect of Lorentz force possibly plays important role in the dynamics of charged dust particles. For the discussion of the effect of Lorentz force in the dust infall problem, we quantitatively evaluate the effect of background magnetic field to the charged dust particle.

By assuming minimum mass solar nebula model and constant plasma beta throughout the disk, we estimate the gyroperiod of charged dust particles. We also assumed the charge state of dust particles by referring the observation result of charged particles in the Saturnian E-ring by Cassini spacecraft [e.g., Horanyi et al., 2004]. For the case that the gyro period approximately equals to the stopping timescale by headwind (e.g., Weidenschilling, 1977) of gas at 1 AU, dust particles with the radius of 1 cm should be charged $\sim 10^{17}$ e (e: elementary charge).

The charge state of dust particles with the radius of 1 μ m measured in the Saturnian E-ring has been reported to 1000 e (e.g., Horanyi, 2004). Assuming that these dust particles collide and coalesce each other and become 1cm sized dust and that the charge state is proportional to its volume, we obtain 10^{15} e for 1 cm dust particles. In the present study, we study the relation between the radius and charge state of dust particles and the validity of the model assumed in the present study for protoplanetary disks so as to discuss electromagnetic effect to the dust particle quantitatively.

Keywords: protoplanetary disk, dusty plasma

Tidal orbital evolution of retrograde hot jupiters

Naoya Okazawa¹, Kiyoshi Kuramoto^{1*}

¹Hokkaido University

Recently, retrograde hot jupiters with orbits run counter to the spin of their central stars have been discovered. For such a hot Jupiter with large orbital inclination, it is hard to think that the planet formed in-situ on a proto-planetary disk or, that it moved to the present position by the interaction with disk gas after planet formation, because the planetary orbit is kept almost align with the disk plane in these processes. Then, the "slingshot scenario" have been proposed as a likely formation scenario of these planets. In this scenario, a gas giant planet with highly elliptical orbit with large inclination has once formed by gravity scattering among gas giant planets formed in a proto-planetary disk. And then, the tidal action of its central star induces the orbital evolution to hot Jupiter.

There remain questions, however, in the processes of such tidal action. For example, tidal action is modelled by assuming dynamical tide in some previous works, because the orbital evolution begins from a highly elliptical orbit (e.g. Nagasawa et al. 2008). However, as the eccentricity becomes small with orbital evolution, it would become appropriate to consider equilibrium tide. In addition, the strength of tidal friction has still been poorly constrained.

This study presents our theoretical analysis of the tidal orbital evolution of six hot Jupiter whose primary stars' ages are known and attempts to estimate likely processes of tidal action and the intensity of tidal friction.

In the tidal interaction, the vector sum of angular momentums of planetary orbit, stellar rotation and, planetary rotation is preserved. Moreover, the angular momentum of planetary rotation is too small to affect the evolutionary pathway. Since the orbital angular momentum of a retrograde planet is always conveyed to that of stellar rotation, the past orbit should have larger angular momentum than the present. That is, the evolutionary pathway kept the current orbital angular momentum has the smallest pericenter distances. For each of the six planets, the time constants of the pericenter passage during such preserving evolutionary pathway are longer than that of planetary free oscillation. This shows that an equilibrium tide model is appropriate for these planets.

By using the equilibrium tide model(Eggleton 1998), numerical calculations of orbital evolution backward in time for the age of each planetary system is performed. Since the tidal dissipation constant which specifies the strength of tidal friction has large uncertainty, it is taken as a parameter. Its value which may reproduce the orbital evolution from an extended elliptical orbit to the present orbit is obtained exploratory.

For each planet, there exists solutions whose early orbit meets the conditions expected from a slingshot scenario (An semi-major axis before the age of a system is 2-3 AU. It does not collide with a central star on the way of orbital evolution). The dissipation constant that agrees with the above conditions can be constrained in a narrow range for each planet. It appears that there is a correlation between planet radius and dissipation constant. The dissipation constant of Jupiter derived from the orbital dynamics of Jovian satellites also follows this correlation.

Using acquired value of dissipation constant, the past tidal heating rate is also estimated. The six retrograde planets may have received tidal heating 0.05-2 times as strong as central star radiation for the earliest billions of years. Furthermore, the orbits of these planets are maintained over the next billions of years or more without falling to the central stars. This would be conformable with the fact that many hot Jupiters exist.

On the magnetic activities in hot Jupiters

Yuki Tanaka^{1*}, SUZUKI, Takeru K.¹, INUTSUKA, Shu-ichiro¹

¹Department of Physics, Nagoya University

Recently theoretical studies on thermal evolution of hot jupiters invoked Ohmic dissipation to account for extraordinary large radii of some objects.

Those analyses suggest the existence of significantly strong magnetic fields in hot jupiters.

To test this hypothesis it is important to investigate possible consequence of magnetic fields in gaseous giant planets.

Since gaseous giant planets are supposed to have large convection zones, magnetic field mediates energy transfer from the interior to the exterior of the atmosphere.

In this talk we develop a model of magnetically driven wind from a gaseous planet and investigate the resultant mass loss.

This work may provide a possible consistency check of theories with observations of hot jupiters.

Keywords: exoplanet, mass loss

Capture and orbital evolution of irregular satellites by gas drag from circumplanetary disk

Ryo Suetsugu^{1*}, Tetsuya Fujita¹, Keiji Ohtsuki¹

¹Dept. Earth Planet. Sci., Kobe Univ.

Many satellites are orbiting about the giant planets in the Solar System. The number of known satellites has been increasing significantly due to advancement of observation technology, and studies of these small bodies help us understand better not only their origin but also formation processes of giant planets. Satellites are classified into regular satellites and irregular satellites. It is thought that regular satellites formed in circumplanetary disks around giant planets, because their orbits are nearly circular and coplanar. On the other hand, orbits of irregular satellites are highly eccentric and inclined, thus, they are thought to be planetesimals captured by the planets through some energy dissipation.

Although several energy dissipation mechanisms for capturing irregular satellites have been proposed by previous works, most of them seem to have difficulty in explaining capture of the irregular satellites of Jupiter. However, Cuk & Burns (2004) argued that a cluster of prograde irregular satellites of Jupiter may be collisional fragments of a single planetesimal captured by gas drag from the circumjovian disk at the final stage of the formation of Jupiter. They integrated orbits of this parent body backward in time, and found that the parent body experienced a period of temporary capture by Jupiter before it became gravitationally bound by Jupiter. If the gas density of the circumjovian disk was too high, a captured planetesimal would likely spiral into Jupiter rather quickly due to large energy dissipation, but its lifetime within the disk is expected to be longer if a gap in the solar nebula was formed by the gravity of Jupiter and the gas density in the circumjovian disk was lower. Therefore, if planetesimals with low energy are temporarily captured by Jupiter for an extended period of time near the end of Jupiter's formation, they may survive for a long time and even weak energy dissipation may be sufficient for capturing them as irregular satellites or their progenitors. However, temporary capture itself has not been examined in detail. Recently we investigated temporary capture of planetesimals by a planet using three-body orbital integration. As a result, we found that temporary capture orbits could be classified into four types and evaluated the rates of temporary capture (Suetsugu et al. 2011 AJ 142, 200; Suetsugu & Ohtsuki, MNRAS, in press).

Growing giant planets can capture planetesimals by gas drag from circumplanetary disk (Fujita et al, submitted to AJ). In order to reveal origin of irregular satellites, it is also important to examine orbital evolution after the capture. In the present work, we will discuss capture and orbital evolution of irregular satellites due to gas drag from circumplanetary disk.

Keywords: planet, satellite